CSIRO PUBLISHING

Australian Journal of Physics

Volume 52, 1999

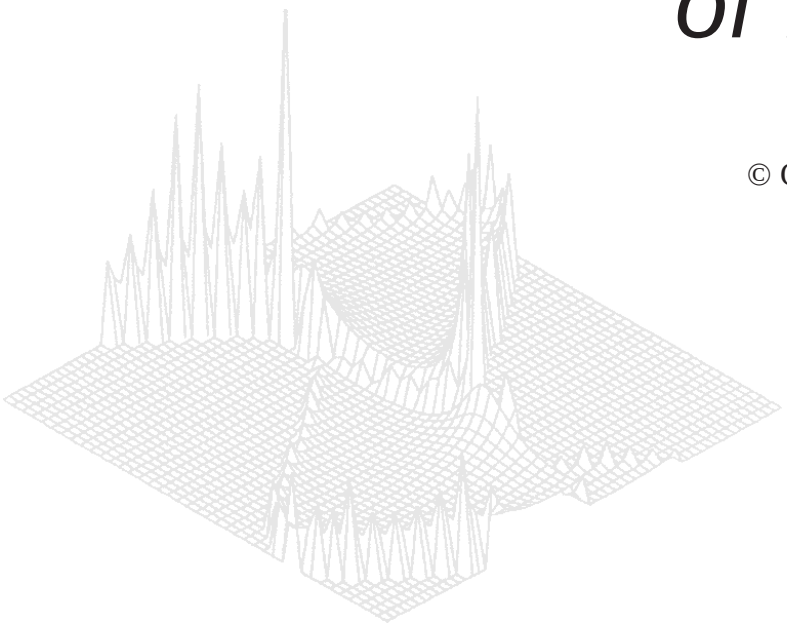

A journal for the publication of
original research in all branches of physics

www.publish.csiro.au/journals/ajp

All enquiries and manuscripts should be directed to
Australian Journal of Physics
CSIRO PUBLISHING
PO Box 1139 (150 Oxford St)
Collingwood Telephone: 61 3 9662 7626
Vic. 3066 Facsimile: 61 3 9662 7611
Australia Email: peter.robertson@publish.csiro.au

Published by **CSIRO** PUBLISHING
for CSIRO Australia and
the Australian Academy of Science

Aust. J. Phys., 1999, **52**, 117–40

Self-assembly, Stability and the Electrical Characteristics of Cell Membranes*

Hans G. L. Coster

Department of Biophysics, School of Physics,
and Centre for Membrane Science and Technology,
University of New South Wales, Sydney, NSW 2052, Australia.

Abstract

Living cells are enveloped in an ultra thin (∼6 nm) membrane which consists basically of a bi-molecular film of lipid molecules in which are embedded functional proteins that perform a variety of functions, including energy transduction, signalling, transport of ions (and other molecules) etc., and also acts as a diffusion barrier between the cell interior (cytoplasm) and the external medium. A simple statistical mechanical analysis of the self-assembly of the membrane from its components provides useful insights into the molecular organisation of the membrane and its electrical properties. The stability of the structure is also closely connected to its electrical properties and this has provided not only a useful tool for fundamental research but has spawned also applications, some of which have had a major impact in biomedical research and are now being exploited commercially. An overview is given of the rapid progress made in our understanding of the physics of both the molecular organisation and function of cell membranes and some of the fascinating and socially and commercially important applications that have flowed from this.

1. Introduction

Membranes play a crucial role in living cells and organisms. For instance, the plasma membranes enveloping living cells separate the exterior, non-living environment from the internal, living, cytoplasm. This membrane provides a selective diffusion barrier to molecules moving into, and out of, the cell. It also contains energy driven transport mechanisms that maintain large concentration differences of many substances between the external environment and the cytoplasm. It is the voltage-gated ion channels in the plasma membrane of nerve cells that generate 'action' potentials which are transmitted along the nerve axons and it is the release of neuro-transmitters at the membrane synaptic junctions which determine the function of the neural networks in the brain. Cells sense the presence of specific molecules in the surrounding medium when these molecules bind to specific receptor molecules embedded in the membrane. Apart from the plasma membrane surrounding the cell, many of the internal organelles are delineated by membranes. Indeed almost all of the biochemical processes in the living cell are associated with membrane bound enzymes and transport and

* Refereed paper based on a plenary lecture presented on 28 September 1998 to the 13th AIP National Congress, held in Fremantle, Western Australia.

 10.1071/PH98088 0004-9506/99/010117$10.00

Fig. 1. An electron micrograph of the plasma membrane (of *Chara corallina*). For the electron microscopy the membrane was 'fixed' by crosslinking using OsO_4 which also enhances the contrast. The two electron opaque bands in its OsO_4 stained structure correspond to the polar regions of the membrane, whilst the central electron-lucent region corresponds to the non-polar, hydrophobic, region (from electron micrograph used in Coster 1973).

transduction mechanisms. An example of an electron micrograph of a plasma membrane is shown in Fig. 1.

The presence of the cell membrane, which is at least two orders of magnitude smaller than the resolution of optical microscopes, was originally inferred from the experimental studies of the permeation of various substances into cells. These indicated that the 'membrane' had lipoidal properties. Interestingly, it was the measurement by Fricke in the 1920s of the impedance of suspensions of cells that provided the first estimate of the capacitance and hence the thickness of the membrane surrounding living cells (Fricke and Morse 1925). Fricke's estimate of 20–30 nm was within a factor of 2 or 3 and no better estimate was obtained until the advent of electron microscopy some thirty years later! (Robertson 1960).

We now know that the cell membrane consists of a bimolecular layer of lipid molecules in which are imbedded a variety of proteins. The bimolecular lipid membrane, also referred to simply as a lipid bilayer, is essentially a 2-D fluid. The lipid bilayer provides a fluid matrix in which the membrane proteins assume specific orientations and form functional aggregates.

We will examine here the statistical mechanics of the assembly of the lipid membranes from its components, the molecular organisation of proteins in the lipid membrane matrix and some of the interesting insights that this can give on the stability and electrical properties of the membranes.

2. The Bi-molecular Lipid Membrane

Lipids are a major component of all cell membranes. There are numerous different kinds of lipid molecules but they all share the feature that they are amphipathic; one region of the molecule is polar and hydrophilic, whilst the other is non-polar and hydrophobic. When dispersed in water these molecules tend to form aggregates. Several forms of the aggregates are possible, depending

on the relative dimensions of the polar head groups and non-polar tails. A lipid commonly found in mammalian cell membranes is phosphotidylcholine (Lecithin) and its structure is shown in Fig. 2.

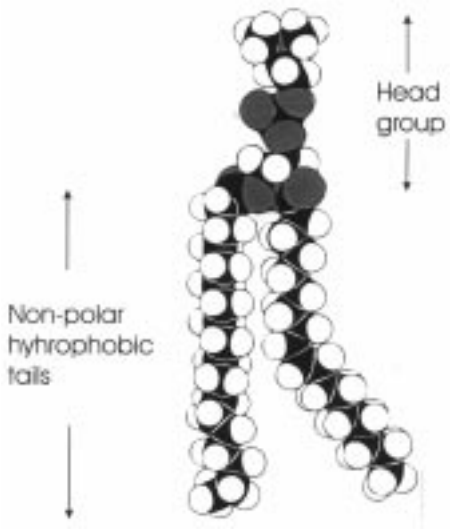

Fig. 2. A 'space filled' model of the lecithin molecule. The polar head region for lecithin contains a zwitterion (trimethyl ammonium-phosphate).

When lecithin is dispersed in water it can form spherical micelles, vesicles and bi-molecular membranes as illustrated in Fig. 3. These aggregates form spontaneously. Indeed on dispersion of the substance in water, the concentration of the monomer initially simply rises with increases in the material added. However, at some stage micelles begin to form and additional lipid added to the mix then does not lead to an increase in the concentration of the monomer molecules; instead the concentration of micelles rises. When the concentration of micelles is sufficiently high, other aggregates such as bi-molecular membrane structures arise. In these bimolecular lipid membranes, the acyl chains of the lecithin molecules which form the hydrophobic interior have a spacing consistent with this region being essentially in a condensed fluid phase. This can be ascertained immediately from low angle X-ray diffraction patterns from liposomes (regular arrays of stacked bimolecular lipid membranes separated by thin regular layers of aqueous solutions). One such diffraction pattern is shown in Fig. 4. The outer diffraction band provides information not only on the spacing but the diffraction band is very broad indicating that the acyl chains are probably moving in the plane of the membrane. This is consistent with NMR measurements which indicate that lateral diffusion of the lipids is similar to that in a fluid, although the structure normal to the membrane is very rigid.

It is interesting to consider the conditions for thermodynamic equilibrium which govern the formation of these structures, their stability and the electrical properties which arise from this.

Statistical mechanical considerations provide the condition for equilibrium between the molecules in the aggregates and the monomers; thus the chemical potential for the molecules in these two states must be the same. The chemical potential will contain terms which are dependent on the concentration or mole-

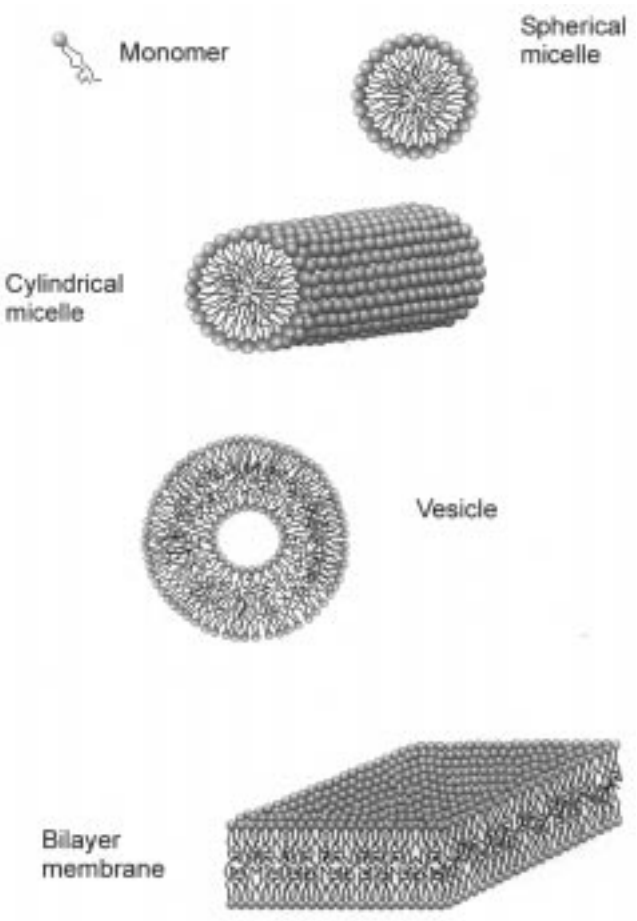

Fig. 3. Some commonly found aggregates of lipids.

fraction of the molecules as well as energy terms which are independent of their concentration. For equilibrium between monomer dispersions of the molecules and say spherical aggregates containing N lipids, we must therefore have

$$\mu_1 = \mu_N \qquad \text{or} \qquad \mu_{1,0} + RT\ln X_1 = \mu_{N,0} + \frac{RT}{N}\ln\frac{X_N}{N}\,, \tag{1}$$

where $\mu_{1,0}$ and $\mu_{N,0}$ are the standard chemical potentials for the monomer and aggregates containing N lipids (N-mers) respectively. These terms include all the contributions which are independent of the concentration. Here X_1 is the mole fraction of the monomers and X_N is the mole fraction of lipids tied up in aggregates containing N lipid molecules; the mole fraction of aggregates, considered as a combined molecular entity is therefore X_N/N. In equation (1) the terms in X represent the entropy, expressed per molecule; for the aggregate (N-mer) this is the 'communal' entropy per molecule.

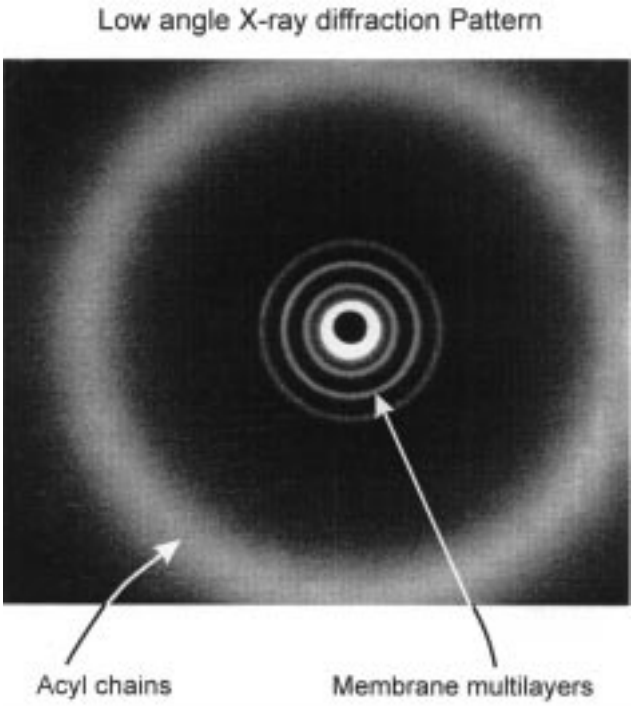

Fig. 4. Low angle X-ray diffraction pattern from a liposome (stacked multiple bimolecular lipid membranes) preparation of lecithin. The broad outer diffraction ring is due to the acyl chains. The smaller (sharper) diffraction rings correspond to the first three orders of the Bragg diffractions from the regularly stacked membranes; with more orders the intensity distribution of these latter diffraction maxima allows the structure, normal to the membrane, to be determined (from experimental diffraction data used in Coster *et al*. 1981).

Consider now the special case of a bi-molecular layer of lipids in equilibrium with the monomers. For the lipid bilayer we wish to explicitly separate out a term in the standard chemical potential which describes the interfacial free energy of the membrane. This is an important parameter in determining the stability and electrical properties of the membrane as we will see later. For a macroscopic piece of a lipid bilayer, N is very large and the entropy term (per lipid molecule) therefore becomes negligible. Thus the equilibrium condition for the lipid bilayer becomes

$$\mu_{1,0} + RT\ln X_1 = \mu_{\mathrm{m},0} + \gamma_{\mathrm{m}} a\,, \tag{2}$$

where γ_{m} is the interfacial free energy per unit area, a is the surface area per molecule and $\mu_{\mathrm{m},0}$ is the standard chemical potential for the lipids in the membrane. For artificially constructed lipid bilayers (e.g. Coster and Simons 1968), γ_{m} is of the order of 1–2 mJ/m^2. This compares with a value of $\sim$50 mJ/m^2 for an oil–water interface.

Electrical Properties

The lipid bilayers have a central, non-polar, layer which is about 2–3 nm in thickness. The partitioning of ions from the aqueous solution into this layer is determined by the Born (1920) energy which derives from image forces which arise as ions approach the membrane which has a hydrophobic region with a very low dielectric constant ($\epsilon_{\mathrm{m}} \sim 2 \cdot 1$; see Fettiplace *et al.* 1971; Coster and Smith 1974; Ashcroft *et al.* 1983) from the aqueous medium which has a dielectric constant, $\epsilon_{\mathrm{w}} \sim 78$. The Born energy for partitioning into the lipid bilayer interior from an aqueous medium is given by

$$W_{\mathrm{B}} = \frac{z^2 e^2}{8\pi\epsilon_0 R}\left[\frac{1}{\epsilon_{\mathrm{m}}} - \frac{1}{\epsilon_{\mathrm{w}}}\right], \tag{3}$$

where R is the radius of the ion, e is the electronic charge, z is the valency of the ions, ϵ_{m} is the dielectric constant of the membrane interior, ϵ_{w} is the dielectric constant for water and ϵ_0 is the permittivity of free space.

For a potassium ion, for instance, the Born energy is of the order of 3 eV. Thus, while the mobility of the ions in the membrane may be quite high, the electrical conductance of the lipid bilayers would be expected to be very low since ion concentration in the membrane will be extremely low. The experimentally measured conductance for artificial lipid bilayer membranes is indeed very low; of the order of 10^{-3} S/m^2, considerably smaller than that of an equivalent layer of glass. The low conductivity of this very flexible, fluid, membrane structure is of significance to the functional properties of the cell membrane. The low conductance of the lipid membranes is, however, several tens of orders of magnitude larger than that expected from the concentration of carriers in the lipid membrane! The explanation for this lies in the formation of pore 'defects'.

Formation of Pore Defects

So far we have considered lipid bilayers which contain no transmembrane connections between the two aqueous phases which it separates. Pore structures can, however, form in the lipid bilayer like that shown in Fig. 5.

The curved surface of the pore is lined with lipid molecules but the packing constraints on the lipid molecules will impose a greater surface area per lipid molecule in these curved regions than in the planar surface of the bilayer itself. Essentially this leads to a greater hydrophobic interaction; the water molecules near the membrane surface will penetrate further into the non-polar constituents of the lipid structure. Indeed it is possible to get a good first approximation of the increase in the surface free energy in these curved regions in the pores from the increased surface area per molecule and assuming a surface free energy per unit area similar to that of an oil–water interface.

Thus, with reference to Fig. 6, for a pore of radius r, the energy required to create the curved surface is

$$W_{\mathrm{p}} = \left(2\pi r \frac{\pi d}{2}\right)\gamma_{\mathrm{p}} = \pi^2 r d \gamma_{\mathrm{p}}\,, \tag{4}$$

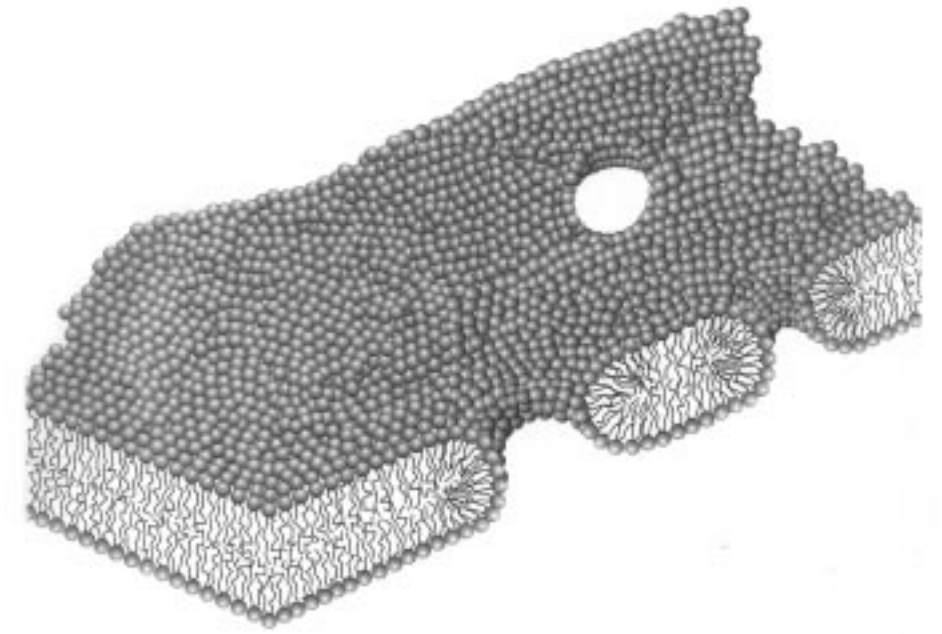

Fig. 5. Annular pores in a lipid bilayer membrane.

where $\gamma_{\rm p}$ is the surface free energy per unit area in the curved regions of the pore.

The energy cost of creating the curved surface of the pore is offset by the energy saved from not forming the disc of planar bilayer where the pore is formed. This latter energy is simply $2\pi r^2\gamma_{\rm m}$. The net cost of creating a pore of radius r is therefore given by

$$E_{\rm p} = \pi^2 r d\gamma_{\rm p} - 2\pi r^2\gamma_{\rm m}\,. \tag{5}$$

Now that we have the energy required to form a pore we can determine, at least the relative, probability of formation of pores of different radii using the Boltzmann distribution function.

These pores will also contribute to the electrical conductance of the membrane. Indeed the conductance of the bilayer itself is so small that the conductance of such membranes is entirely due to that of the pores. The conductance of a pore filled with water will depend on the radius of the pore as well as the concentration of ions. The latter will continue to be influenced by image forces due to the surrounding lipid bilayer and will depend on the shape of the pore. For simple geometries such as a cylindrical pore, the Born energy for partitioning can be readily determined (Parsegian 1969) and for a long and narrow pore is given by

$$W_{\rm B} = \frac{z^2e^2\alpha}{4\pi r\epsilon_0\epsilon_{\rm w}}\,, \tag{6}$$

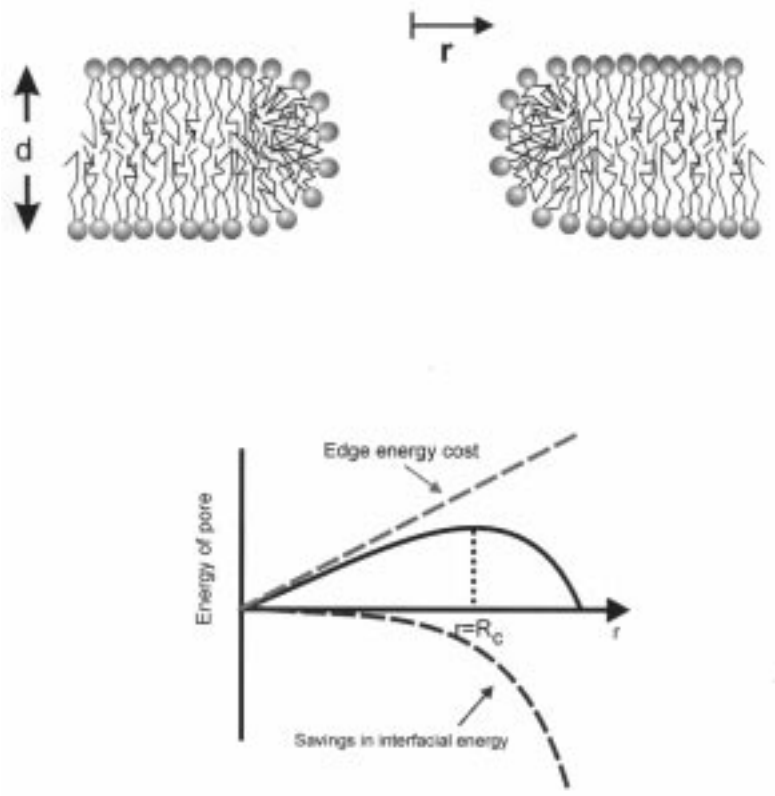

Fig. 6. Cross section of a pore in the bilayer and the contributions to the energy of formation of such a pore as a function of its radius. The net energy to form a pore has a maximum at $r = R_C$. Pores larger than R_C will grow larger uncontrollably.

where z is the valency of the charge carriers (ions), e is the electronic charge, α is a form factor and for a cylindrical pore has a value of $0{\cdot}175$ (Parsegian 1969), r is the radius of the pore, ϵ_w is the dielectric constant of water and ϵ_0 is the permittivity of free space.

The total conductance of the membrane will, of course, also depend on the total number of pores. These two factors can be separated experimentally by measurement of the activation energies for electrical conduction. An example of this (from Smith *et al.* 1984) is shown in Fig. 7. The activation energies for conduction in these particular lipid bilayers (2 : 1 Lecithin : Cholesterol) had a value of ∼38 kJ/mole.

This activation energy for conduction contains a contribution due to the activation energy for diffusion through the aqueous medium in the pore (∼18 kJ/mole). The remaining 20 kJ/mole of the energy of activation contains two components:

(i) the Born energy of partitioning of the ions into the pore (image forces);
(ii) the temperature dependence of the average pore size (and perhaps the number of pores).

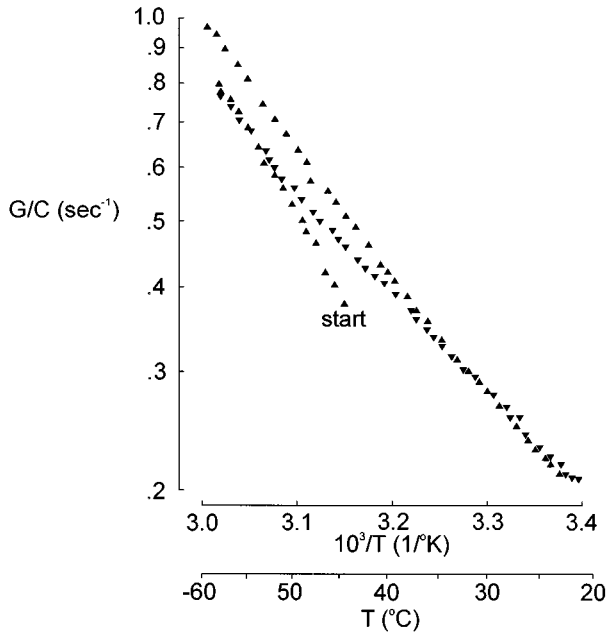

Fig. 7. An Arrhenius plot of the conductance, normalised with respect to the capacitance (and hence membrane area), of a lecithin-cholesterol lipid membrane in a 1 mMKCl solution. The triangles and inverted triangles refer to measurements whilst the temperature was rising and falling respectively. The final slope of this plot yields an activation energy for conduction of 38 kJ/mole (from Smith *et al.* 1984).

It is difficult to separate these two contributions. A lower limit on the *average* pore size may be obtained by assuming the activation energy to derive solely from the Born image forces. On the further assumption that the diffusion of ions in the pore is the same as that in the free solution (mobility $\sim 2\times 10^{-9}$ m^2/s) and using the value of the partition coefficient for the ions determined by the Born energy (equation 6), the radius of an equivalent cylindrical pore and its conductance then can be calculated. From this we can also calculate the total number of pores. This yields the following values: pore radius of $\sim 1\cdot 1$ nm and number of pores per m^2 of $\sim 10^{10}$. Though the pores completely determine the electrical conductance, they occupy only 2×10^{-7} of the total area and will contribute negligibly to the hydraulic permeability of the membrane.

Membrane Stability

From equation (5) (see also Fig. 6), the maximum energy for the formation of a pore (when $\partial E_{\mathrm{p}}/\partial r = 0$) occurs at a radius R_{c} given by

$$R_{\mathrm{c}} = \frac{\pi d \gamma_{\mathrm{p}}}{4\gamma_{\mathrm{m}}}\,, \tag{7}$$

and the energy of such a pore is given by

$$E_c = \frac{\pi^3 (d\gamma_p)^2}{8\gamma_m} . \tag{8}$$

The radius R_c is a *critical* radius because a pore of that size will spontaneously grow and this would rupture the membrane. In a cell this would cause lysis of the cell.

Lipid molecules which have a smaller volume of non-polar components or relatively larger polar heads would be expected to pack more favourably into the curved region of the pore. This would decrease the surface free energy in the curved surface of the pore, and hence decrease the critical pore energy and critical pore radius. It is interesting to note that there exists a form of lecithin which has only one hydrocarbon-chain tail but the same polar head group (trimethyl ammonium-phosphate). This lipid would favour the formation of pores and it is interesting to note that this lipid promotes the lysis of cells and is in fact known as *lysolecithin*. Conversely, molecules such as cholesterol, which have a very small polar head (a single OH group) and a bulky hydrophobic part, would inhibit the formation of pores. Indeed, in experimental studies on lipid bilayers, the addition of cholesterol to bi-molecular membranes of lecthicin greatly increases the stability of such membranes. Cholesterol is found in all mammalian cell membranes.

Effect of Trans-membrane Potentials on Pore Defects

Living cells maintain an electric potential difference between the cell interior (cytoplasm) and the external medium. This potential difference varies from ∼10 mV in erythrocytes (red blood cells) to >250 mV in some aquatic plant cells. The interior of the cell is always negative with respect to the external medium. This potential difference appears across the cell membrane and is usually simply referred to as the membrane potential. If we take a value of 60 mV as typical (e.g. neurones), this potential difference across a membrane which is ∼6 nm thick represents an average field strength in the membrane of $\sim 10^7$ V/m, a truly large field strength. Further, the field strength in individual regions of the membrane, and in particular the central region, is likely to be an order of magnitude larger than this average value.

Electrical Energy Stored

With field strengths this large we must take into account the electrical energy stored in the membrane when considering its molecular organisation and stability. The membrane capacitance is typically around 10^{-2} F/m^2 (Fettiplace *et al.* 1971; Coster and Smith 1974) so the electrical energy stored at a membrane potential of 60 mV is $\sim 1{\cdot}8\times 10^{-5}$ J/m^2. That value is considerably smaller than the $1\text{–}2\times 10^{-3}$ J/m^2 for the interfacial free energy. As we shall see, however, the electrical energy stored may be of significance in the energy of formation of the pores.

We will initially restrict ourselves to pores which are small compared to the Debye length for the surrounding medium. In that case the potential difference appearing across the membrane will not substantially collapse in the area occupied

by the pore. The pore, however, is filled with an aqueous medium with a dielectric constant of ∼78, whilst the interior of the membrane has a dielectric constant of ∼2·1. The formation of a pore therefore will lead to a change (increase) in the charge stored. The *free energy* of the system, however would then *decrease* as the charging is driven by the emf generated as a result of differences in the ionic composition of the internal and external media.* These concentration and composition differences are maintained via energy-driven ion 'pumps' located elsewhere in the membrane. Another way of looking at the process (illustrated in Fig. 8) is that, in the presence of a potential difference across the membrane, water is drawn into the pore since its dielectric constant is higher than that of the membrane and this process is opposed only by the net energy costs of creating the pore in the membrane due to interfacial free energy terms.

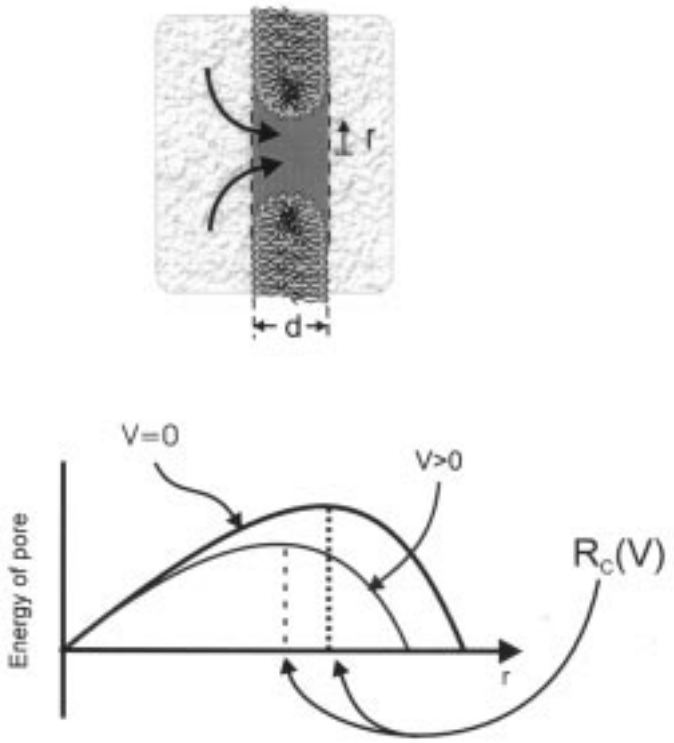

Fig. 8. Effect of transmembrane potential on the critical pore radius. The application of a transmembrane potential will cause the pore in the membrane (which has a low dielectric constant) to enlarge as water with a dielectric constant of 78 is drawn into the pore. The critical radius of a pore, for which the energy of formation is a maximum, decreases in the presence of a transmembrane potential.

The energy of a pore of radius r (assumed to be much less than a Debye length), in the presence of a membrane potential V_{m}, is therefore given by

$$E_{\mathrm{p}} = \pi^2 r d\gamma_{\mathrm{p}} - 2\pi r^2 \left(\gamma_{\mathrm{m}} + \frac{C_{\mathrm{m}} V_{\mathrm{m}}^2}{2}\right), \tag{9}$$

* The charging of a capacitor from a battery decreases the overall energy in the system which comprises the battery plus the capacitor, though the energy stored in the capacitor increases.

where C_{m} is the membrane capacitance (per unit area) and V_{m} is the transmembrane potential. The critical radius when $\partial E_{\mathrm{p}}/\partial t = 0$ is then

$$R_{\mathrm{c}} = \pi d\gamma_{\mathrm{p}} \Big/ 4\left(\gamma_{\mathrm{m}} + \frac{C_{\mathrm{m}} V_{\mathrm{m}}^2}{2}\right). \tag{10}$$

The energy to form such a critical pore is then given by

$$E_{\mathrm{c}} = \pi d\gamma_{\mathrm{p}}^2 \Big/ 8\left(\gamma_{\mathrm{m}} + \frac{C_{\mathrm{m}} V_{\mathrm{m}}^2}{2}\right). \tag{11}$$

The critical radius and the energy to form such a critical pore, which would lead to rupture, is decreased (see Fig. 8) and the probability of such a pore forming (via the Boltzmann probability function) thus will rapidly increase with increasing membrane potential. At sufficiently large membrane potentials the probability of a critical-radius pore forming rises significantly.

For large pores (with a radius much larger than the Debye length) the membrane potential difference in the central portion of the pore will collapse and there will not be a contribution to the electrical energy of the pore from these central regions. However, the peripheral region of the pore (within a Debye length of the perimeter) will continue to contribute to the free energy as before, although the functional dependence on the radius will then vary as r and not as r^2.

3. Proteins in Membranes

The plasma membrane of cells also contains a variety of proteins which perform various specific functions; these are the nano-machines which physically move ions and other molecules against their chemical gradients, generate electrical signals and perform a complex variety of recognition and sensing functions.

Elementary statistical-mechanical considerations of the organisation of these proteins in the lipid bilayer matrix provide some insights into the electrical characteristics of the cell membrane and its relation to the functional properties of the proteins and possible sensing mechanisms. We have already pointed out that the lipid bilayer membrane is an extremely good electrical insulator, despite the presence of pore 'defects'. The electrical properties of cell membranes is dominated by the proteins imbedded in the lipid bilayer. The latter, however, plays a very important role in the organisation of the proteins and the latter features strongly in the electrical characteristics.

Many functional membrane proteins are composed of subunits (often six) which span the membrane and are connected by flexible strands which remain external to the membrane. The positioning and axial orientation of the proteins results from a balance between opposing hydrophobic and hydrophilic forces between the aqueous environment, the non-polar membrane interior and the polar and non-polar portions of the protein. The detailed structures for some of these proteins are now known, for others the amino acid sequence allows one to determine which portions will be held in the membrane and which will protrude into the aqueous media on either side.

Protein Aggregation

For a protein to span the entire lipid membrane the protein needs to have a central non-polar region that matches the central hydrophobic region of the lipid bilayer and polar regions which protrude into the aqueous environments (e.g. see Singer and Nicholson 1972). A mismatch, for instance between the dimensions of the non-polar region of the protein and the non-polar region of the lipid bilayer, will be associated with a hydrophobic interaction energy. The latter will depend on the detailed structure of the protein. For many proteins this structure is now known and it is possible, although not trivial, to evaluate the interaction energy. To gain insights into the physics of this problem we can

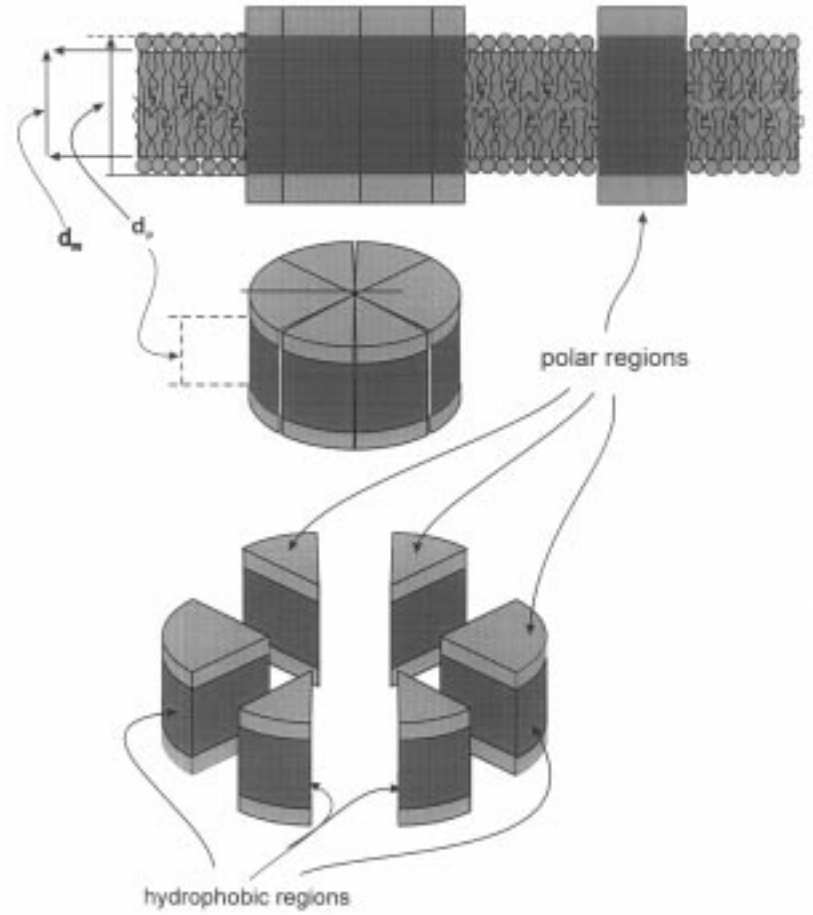

Fig. 9. A hypothetical protein module consisting of six subunits, imbedded in a lipid bilayer membrane. The subunits may either be dispersed as single subunits or may aggregate as hexamers. The statistical-mechanical equilibrium distribution of these configurations is determined by the chemical potentials of the monomer and hexamers. The latter includes hydrophobic energy terms arising from geometrical mismatches between the hydrophobic region of the lipid bilayer matrix and that of the proteins. Such mismatches tend to favour the formation of the aggregates.

begin by noting that for those parts of the protein which have a hydrophobic surface the interaction energy will be similar to that of an oil–water interface, that is ∼50 mJ/m^2 (Israelachvili 1977). Interestingly, a mismatch might induce the aggregation of the protein subunits if that results in a reduction in the area of contact between the mismatched protein and the non-polar regions of the bilayer (Israelachvili *et al.* 1976). For example, consider the hypothetical protein subunits shown in Fig. 9.

Here it is assumed that the non-polar region of the central portion of the protein subunits do not match (are larger) than the thickness of the non-polar region of the lipid bilayer. All the subunits, however, match each other. The hydrophobic interaction energies will then be different for the aggregated and separated subunits. We will denote this difference as $E_{\rm h}$. The statistical equilibrium between aggregates of the six subunits (hexamers) and the dissociated units (monomers) is determined by the requirement that the chemical potentials for these configurations to be the same (see also Coster 1990). Thus, we have

$$\mu_{1,0} + kT\ln X_1 + E_{\rm h} = \mu_{6,0} + \frac{kT}{6}\ln\frac{X_6}{6}\,, \tag{12}$$

where $\mu_{1,0}$ and $\mu_{6,0}$ represent the standard chemical potentials and contain the contributions which are not dependent on the concentration, including the hydrophobic interactions between the protein subunits and the lipid bilayer when it is in the hexamer configuration. In that configuration the flat faces of the protein subunits only interact with each other and, as the non-polar regions match, this does not involve additional hydrophobic interactions. For the monomer subunits, however, these protein surfaces are exposed to the lipid bilayer matrix which they do not match. This additional interaction energy is designated $E_{\rm h}$ and explicitly included as a separate term. Apart from this difference in the hydrophobic interaction energy, the interactions with the bilayer matrix of the monomer and the individual subunits in the hexamer aggregate are identical in this simple hypothetical example.

Even for very small mismatches this energy difference can be substantial. For the particular example shown in Fig. 9, with a hydrophobic region $d_{\rm m} = 2{\cdot}00$ nm for the lipid bilayer and a value of $d_{\rm p} = 2{\cdot}01$ nm for the hydrophobic region of the protein subunits, this difference corresponds to ∼0·15 eV (or ∼6·3 units of kT at room temperature).

The ratio of hexamers to monomers can then be obtained directly using the Boltzmann distribution function. Thus taking $\mu_{1,0} = \mu_{6,0}$ the ratio of hexamer aggregates to monomers is given by

$$X_6/(X_1)^6 = {\rm e}^{6E_{\rm h}/kT}\,. \tag{13}$$

For the case in question, essentially all the proteins will be in the hexamer forms; for 10^5 hexamers the ratio of hexamers to monomers will be $5{\times}10^4$.

Effect of Membrane Potential and Homeostasis

It has been suggested (Coster and Zimmermann 1975*b*; Zimmermann *et al.* 1977; Coster *et al.* 1980) that the extremely high electric field strengths in the

membrane may give rise to electrostriction effects in the proteins in the membrane. This can have profound effects on the molecular organisation of the proteins (e.g. Coster 1990). This may be illustrated by considering the effect on the protein subunits shown in Fig. 9. The intense electric fields in the membrane will cause a compression of these proteins. The compression will be largely confined to the non-polar parts of the proteins since most of the field appears across the non-polar part of the membrane. The compression of the proteins due to the field can be obtained by considering the balance between the elastic (mechanical) restoring force per unit area P_{m} and the stress P_{e} due to the electric field (Coster and Zimmermann 1975*b*). Assuming, for simplicity, that the proteins continue to behave as an ideal elastic material even when the deformations are very large, we then have for the elastic restoring force per unit area

$$P_{\mathrm{m}} = Y \int_{d_0}^{d} \frac{\mathrm{d}x}{x} = Y \ln \frac{d}{d_0} \,.$$

Here d and d_0 are the thickness of the non-polar portion of the protein subunits with and without the field respectively; Y is the elastic modulus of the proteins. The electric stress per unit area is given by

$$\tfrac{1}{2}\epsilon_{\mathrm{p}}\epsilon_0 E^2 = \tfrac{1}{2}\frac{\epsilon_{\mathrm{p}}\epsilon_0 V_{\mathrm{m}}^2}{d^2} \,,$$

where E is the electric field strength in the protein module and $\mathrm{e_p}$ is the relative dielectric constant of the protein.

At equilibrium the electric field stress is balanced by the mechanical restoring force, that is $P_{\mathrm{e}} + P_{\mathrm{m}} = 0$, and hence

$$\frac{\epsilon_{\mathrm{p}}\epsilon_0 V_{\mathrm{m}}^2}{2d^2} = Y \ln \frac{d_0}{d} \,. \tag{14}$$

As the membrane potential difference is increased, the non-polar parts of the protein subunits will compress and eventually will match that of the lipid bilayer membrane, d_{m}. At that point the energy of the aggregated (hexamer) and monomer proteins are identical and the entropy term in equation (12) will lead to a predominance of the monomer configuration over the hexamer configuration. If the trans-membrane potential difference is increased further, the proteins will be further compressed and the non-polar regions of the proteins will then become smaller than the non-polar region of the lipid bilayer and this will once again lead to a difference between the free energy of the monomers and that of the hexamer aggregate.

This will then again lead to an increase in the proportion of hexamers compared to monomers. Assuming that the interaction energy between the polar parts of the protein and the non-polar part of the lipid bilayer (which they will now protrude into) is again similar to the oil–water interface, we can then determine the proportion of hexamers to monomers. An example of the variation of this ratio as a function of membrane potential is shown in Fig. 10. For the purpose of this calculation the dimensions of the non-polar region of the protein subunits were

set equal to the bilayer membrane thickness d_m, when the membrane potential is equal to 65 mV. At membrane potential smaller or larger than this the protein will then mismatch the bilayer. Functional proteins such as ion 'pumps' are involved in maintaining ion concentration differences which in turn determine the membrane potential. In addition some of these ion pumping mechanisms involve a net charge transfer (electrogenic transport). If the protein has to be in the hexamer configuration for the transport mechanism to function, then we can see that the dependence of the aggregation on membrane potential by the mechanisms outlined provide a homeostatic control system that will maintain a set membrane potential. The latter is of importance in controlling the amplitude of nerve impulses (action potentials) and muscle contractions, etc. The membrane potential also plays a central role in determining the thermodynamic potentials that drive the synthesis of ATP (adenosine triphosphate) from proton gradients across membranes.

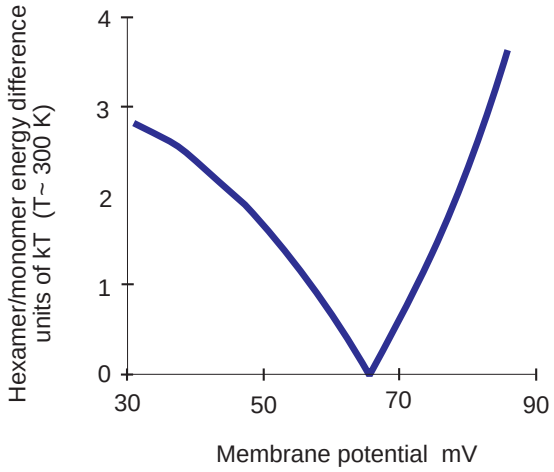

Fig. 10. Differences in energy (per monomer) between the hexamer aggregate and individual monomers, as a function of membrane potential for the hypothetical protein, shown in Fig. 9. For this illustration the hydrophobic region of the uncompressed protein module was set to $2{\cdot}2$ nm, the bilayer hydrophobic region to 2 nm, the elastic modulus of the protein to 10^6 N/m^2 and the dielectric constant of the protein to 20. The hexamer aggregate had a radius of 6 nm. Note that at a membrane potential of ~65 mV (typical of the membrane potential in living cells), the difference in the hydrophobic energies of interaction with the bilayer for the hexamer and monomer configurations are the same. The hexamer form will then not be favoured.

4. Electrical Breakdown in Cell Membranes

We noted earlier that the electrical energy stored in the membrane capacitance is small, at typical values of the membrane potential (~70 mV), compared to the interfacial free energy of a bimolecular lipid membrane (~25 μJ/m^2 compared to 1–2 mJ/m^2). However, at a membrane potential of 700 mV, the electrical energy stored is comparable to the interfacial free energy. This would immediately suggest that at such large trans-membrane potentials the membrane might become unstable. We examined some of the mechanisms that might lead

to such instabilities. The electrical properties of the cell membrane for most cells can only be measured indirectly as the cells are too small to insert electrodes into the cells to measure directly membrane potentials or to inject current. There exist, however, fortunately, some cells which are larger and which make it possible to insert microelectrodes to make direct measurements of the electrical characteristics of the cell membranes. The set-up for this is shown in Fig. 11 (after Coster and Zimmermann 1975*a*). The microelectrodes are typically hollow glass pipettes filled with a salt solution (e.g. 3M KCl). The electrode tips have diameters of 1–10 μm.

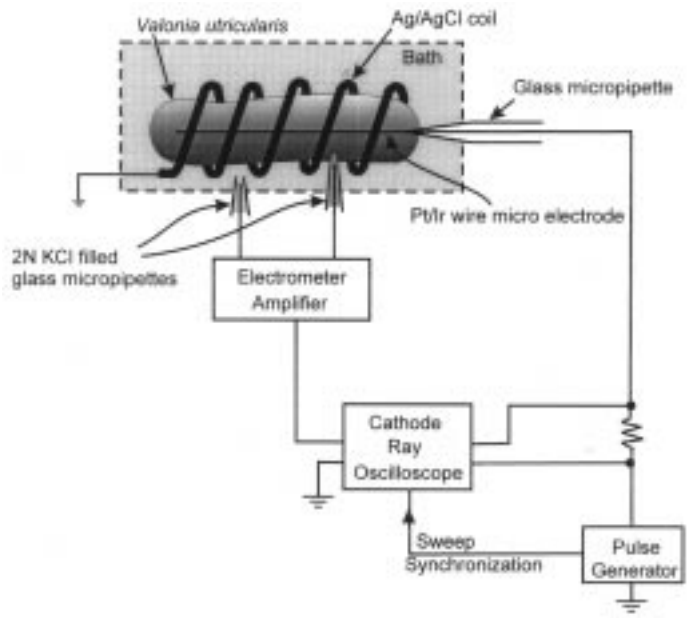

Fig. 11. Diagrammatic set-up for measuring V–I curves (based on Coster and Zimmermann 1975*a*). The KCl filled glass micropipette electrodes had tip diameters of $\sim$5 μm and were used to measure the transmembrane potential. Current pulses were injected via the intracellular Pt/Ir electrode which was inserted via a glass micropipette inserted longitudinally into the cell.

An example of the voltage–current relationship is shown in Fig. 12 (from Coster and Zimmermann 1975*a*). Electrical breakdown of the cell membrane is clearly demonstrated in this case. It is interesting to note that the breakdown in this case does not cause destruction of the cell. If the breakdown occurs via the formation of critical pores in the lipid bilayer matrix, the growth of such pore defects in the cell membrane is pinned by the presence of proteins.

Another possibility is that breakdown occurs at these large transmembrane potentials by electrostriction of the proteins imbedded in the membrane. Thus in a protein module the electrostriction varies as the square of the field strength. The field strength, of course, depends on the thickness of the protein module itself and this decreases with increasing membrane potential. The electrostrictive force therefore varies as the square of the changes in the dimension of the module

while the elastic restoring forces that balance the electrostriction will, ideally, vary only logarithmically. This can clearly lead to a critical point where the electrostrictive compression leads to a catastrophic collapse of the protein when it can no longer be held as an integral part of the membrane.

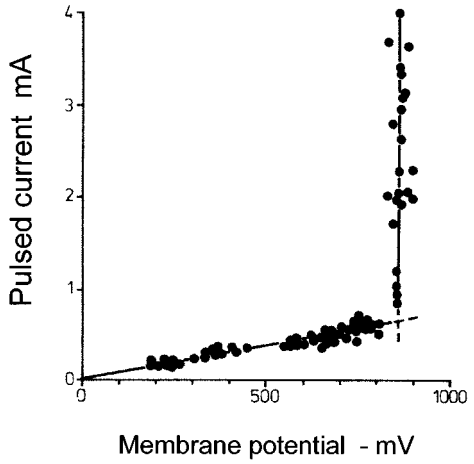

Fig. 12. Voltage–current curve for 1 mS pulse currents in the membrane of *Valonia utricularis*. The data points shown were *not* obtained in order of increasing potential. The electrical breakdown which produced the rapid rise in the current with potential at 850 mV did not lead to irreversible damage to the cell membrane and the characteristics were very reproducible. This was the first direct demonstration of electrical breakdown in the voltage–current characteristics of cell membranes (redrawn from Coster and Zimmermann 1975*a*).

The critical potential for this is given by (Coster and Zimmermann 1975*b*)

$$V_{\mathrm{c}} = \left[\frac{0{\cdot}3679 Y d_0^2}{\epsilon_{\mathrm{p}}\epsilon_0}\right]^{\frac{1}{2}}, \tag{15}$$

where Y is the elastic modulus of the membrane, ϵ_{p} is the dielectric constant of the protein, ϵ_0 is the permittivity of free space and d_0 is the uncompressed thickness of the module. In this model, one would expect the critical breakdown potential to vary with temperature through the temperature dependence of the elastic modulus. Indeed, this is the case as shown in Fig. 13 (from Coster and Zimmermann 1975*b*).

Note that the breakdown potential decreases with increasing temperature, indicating that the elastic modulus decreases with increasing temperature which indicates that the elastic properties are determined predominantly by the energetics of deformation of the protein and that the configurational entropy is not as important (that is, the modules do not behave as entropy springs!). It is worth noting the rather good agreement between the experimental data and the electrical characteristics predicted by this simple model; once the breakdown potential is

fed into the model, the model on which theoretical curves shown in Fig. 13 are based has no adjustable parameters.

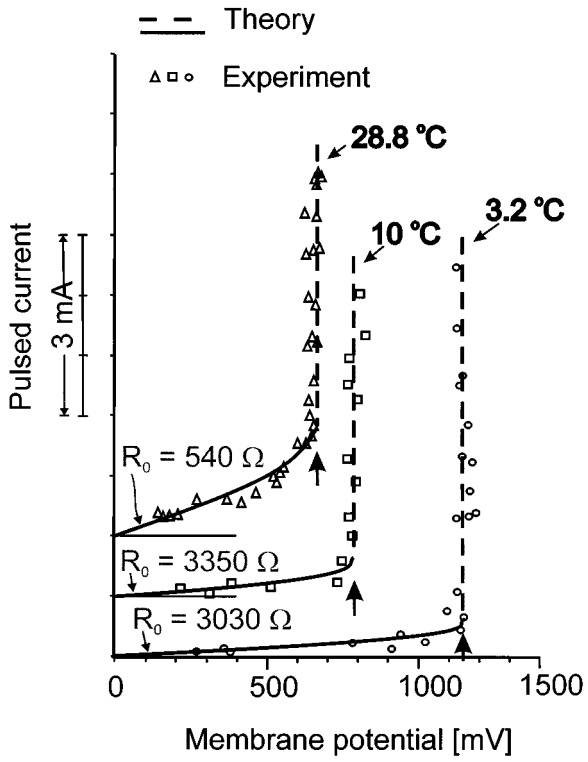

Fig. 13. Voltage–current plots for pulsed (0·5 mS pulses) currents for a cell of *Valonia utricularis*, at various temperatures. The experimental points on these plots were *not* taken in order of increasing current; they were measured in random order. The theoretical curves were obtained assuming the conduction modules in the membrane undergo electrostriction. Apart from the critical membrane potential for electrical breakdown, which is determined from these plots, the theory has no other adjustable parameters (redrawn from Coster and Zimmermann 1975*b*).

5. Practical Applications

The electrical properties of cell membranes and their relation to the molecular organisation of the membrane has provided us with new insights into the complex transport, sensing and signalling functions of living cells. These insights have also led to practical applications which have important social and commercial implications. We will examine just a few below.

Electrical Breakdown of Cell Membranes

The electrical breakdown phenomenon has provided an interesting tool for the study of the electro-mechanics of cell membranes. The breakdown characteristics may also provide a new tool for diagnostic purposes. Thus the breakdown potential as well as the electrical characteristics near the breakdown potential

differ for different types of cells and vary with the state of the cell and it may be a useful tool for monitoring progressive changes occurring in cells (such as erythrocytes) in certain diseases.

Another application of the controlled electrical breakdown of the cell membrane is to produce large, transient, changes in the permeability of the cell membrane. Of particular interest here is the possibility to induce transient permeability to macro-molecules, including strands of DNA. The induction of these transient permeability states by electrical breakdown is known as 'electroporation' and is now a common, and almost essential, tool for genetic engineering; there are dozens of manufacturers of electroporation equipment.

Electroporation is also being used to enhance the take up of drugs in topical applications of drug via 'patches'; usually the uptake of drugs, without electroporation, from impregnated patches placed on the skin is very slow and this otherwise limits the use of this method.

Cell Dielectrophoresis

Particles placed in a uniform alternating electric field will distort the field in their vicinity. The field distortion will depend on the geometry as well as the conductance and dielectric constant of the particle and that of the surrounding fluid. Living cells have an interior (cytoplasm) which has a high conductivity (due to an accumulation of ions such as K^+) and an average dielectric constant a little lower than that of surrounding aqueous medium. The cell membrane, as we have seen, has a very low electrical conductance and a very high area specific capacitance ($\sim$10 mF m^{-2}), although it has a low dielectric constant. When placed in a uniform AC electric field, the manner in which a living cell distorts the electric field will be a strong function of the frequency of the applied field. At very low frequencies, the field will be largely excluded from the cell as the membrane impedance is very high; the instantaneous induced dipole in the cell is then usually in the direction opposite to the field. At higher frequencies, the reactive impedance of the membrane becomes small compared to the conductance of the cytoplasm and the field penetrates the cell; the induced dipole is then in the same direction as the field and usually of larger magnitude than at very low frequencies. At still higher frequencies the field pattern is essentially independent of the conductance (of the cell, membrane or external medium) since the current flowing is dominated by the displacement current and the movement of charge carriers becomes relatively negligible. This is the 'optical' region and for living cells in appropriate aqueous media this occurs at frequencies of tens of mega Hertz. The instantaneous induced dipole is then again in the opposite direction to the applied field. The field patterns around a cell in these three frequency regions is illustrated qualitatively in Fig. 14.

The polarisation or complex dielectric constant of a cell is therefore a complex, and usually a tri-phasic, function of the frequency (Mahaworasilpa *et al.* 1994). Each cell type has a characteristic polarisation-frequency 'signature'. In non-uniform applied AC fields a cell will experience a force whose magnitude and direction will vary in a complicated manner with the frequency of the applied field. This effect can be exploited to selectively manipulate cells using AC electric fields applied via suitable micro-electrodes. The movement of particles in AC electric fields is referred to as 'dielectrophoresis' and is independent of any net

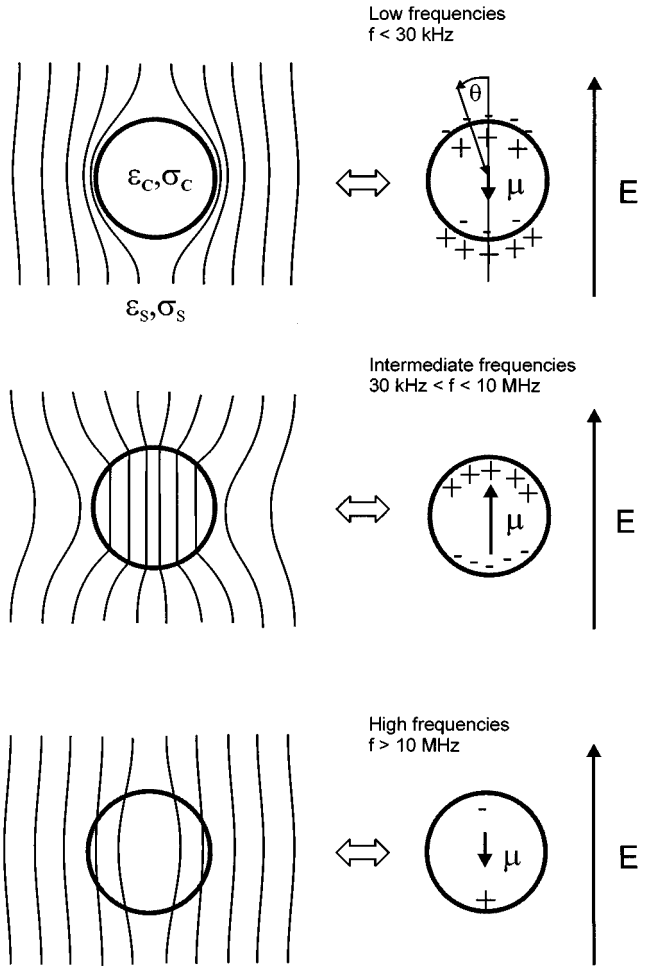

Fig. 14. Electric field patterns around a living cell for three different frequency regimes. The membrane surrounding the cell is a very poor conductor but has a high capacitance. The cell interior (cytoplasm) is a very good conductor. At low frequencies, therefore, the field does not penetrate the cell (because the membrane acts as an insulator) whereas at higher intermediate frequencies the membrane capacitance has a very low impedance and the field then penetrates the cell interior. At very high frequencies the electrical conductance becomes unimportant because the displacement current is dominant and the field pattern is determined by the dielectric structure; this is the 'optical' region.

charge on the particle (in contrast with electrophoresis which occurs in DC fields and is dependent on the charge). The dielectrophoretic force can be readily measured and can be used to characterise cells as well as to separate different cells from each other. The latter is most easily achieved by constructing a track of electrodes which are connected to signal generators (with suitable relative phase shifts) to produce a travelling wave along the track (see Fig. 15). Cells placed on these tracks will then move along the track at a speed (and direction)

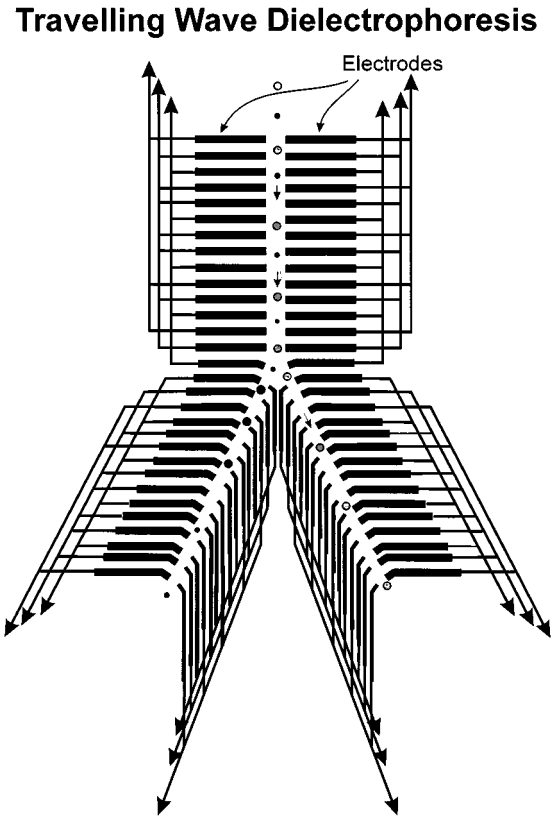

Fig. 15. A track of electrodes in which the phase of the AC signals applied to adjacent electrodes is incremented by 90° to produce a traveling wave. Cells placed on such a track can be levitated by negative dielectrophoresis (repelled from the high field regions near the electrode) and then moved along the track. The speed of movement and at appropriate frequencies even the direction of movement will generally be different for different cells. With a branch track of electrodes energised at a different frequency it is possible to sort different cells by appropriate choice of frequencies of the fields (based on Pethig and Markx 1997).

determined by their frequency dependent polarisation (e.g. see Pethig and Markx 1997; Markx *et al*. 1994; Markx and Pethig 1995). It is thus possible to construct micro-chip cell sorters.

Cell Electrofusion

Controlled electroporation can also be used to cause two cells, brought into close contact, to fuse with each other. The trick here is to use radio frequency electric fields to bring the cells together by positive dielectrophoresis and then induce electrical breakdown in the two cell membranes at their point of contact; this is an electrically induced reverse-mitosis. This technique has now been perfected and has opened up the possibility of creating hybrid cells that have a genetic make-up which is a combination of that of the two cells that were fused.

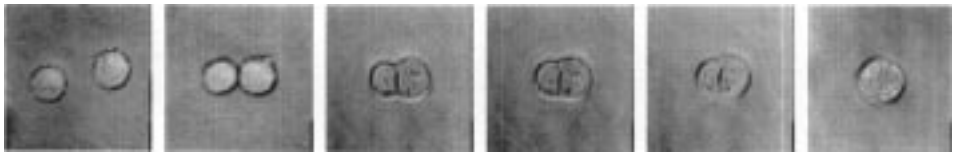

Fig. 16. A sequence of photomicrographs showing two cells being manipulated using dielectrophoresis to form a pair which is tightly apposed (Coster, Monaghan and Mahaworasilpa 1996 unpublished results, courtesy FuCell Pty Ltd, Sydney). The cells were then fused at their point of contact using carefully controlled electroporation (panel 3 from left). The two cells then gradually merge (panels 3–5) and the resulting hybrid cell (last panel) eventually went on to divide.

New cell types of almost any species, or even cross species, can be, and have been already, created in our laboratory. In particular, this technique can be used to create a hybrid cell from a lymphocyte that is secreting antibodies to, say the Hepatitis B virus, and a cancer cell (which is essentially immortal and continues to divide regularly under appropriate conditions). Such a hybrid cell, called a hybridoma, can be grown in culture indefinitely for the production of the antibodies. The original lymphocyte on the other hand cannot be cultured indefinitely as it divides only a few times (that is, it is mortal). The antibodies so produced in culture can be used to treat patients infected with the virus (which is targeted by the antibodies). The creation of mouse hybridomas was developed by Koehler and Millstein in the 1970*s* (for which they received the Nobel prize), but the chemical technique they developed (and all the modifications of that basic method up till now) has proved unsuitable for the generation of human hybridomas that would produce human antibodies; mouse antibodies cannot be used therapeutically in humans because our immune system mounts an severe immune response to such molecules as they are 'foreign' to our system. We have been able in our laboratory to produce stable, antibody secreting human hybridomas using the dielectrophoretic-electrofusion technique. A sequence of photo-micrographs showing the dielectrophoretic manipulation of two cells to form a pair and their subsequent electro-fusion is shown in Fig. 16. The pharmaceutical products derived from such cells are likely to be entering clinical trials in two years.

References

Ashcroft, R. G., Coster, H. G. L., Laver, D. R., and Smith, J. R. (1983). *Biochim. Biophys. Acta* **730**, 231–8.

Born, M. (1920). *Z. Phys*. **1**, 45–8.

Coster, H. G. L. (1973). *Biophys. J*. **13**, 1119–23.

Coster, H. G. L. (1990). *In* 'Electropharmacology' (Eds G. M. Eckert *et al.*), pp 139–58 (CRC Press: Boca Raton, USA).

Coster, H. G. L., and Simons, R. (1968). *Biochim. Biophys. Acta* **163**, 234–9.

Coster, H. G. L., and Smith, J. R. (1974). *Biochim. Biophys. Acta* **373**, 151–64.

Coster, H. G. L., and Zimmermann, U. (1975*a*). *Z. Naturforsch*. **30c**, 77–9.

Coster, H. G. L., and Zimmermann, U. (1975*b*). *J. Membrane Biol*. **22**, 73–90.

Coster, H. G. L., James, V. J., Berhet, C., and Miller, A. (1981). *Biochim. Biophys. Acta* **641**, 281–5.

Coster, H. G. L., Laver, D. R., and Smith, J. R. (1980). *In* 'Bioelectrochemistry' (Eds H. Keyzer and F. Gutmann), pp. 331–52 (Plenum: New York).

Fettiplace, R., Andrews, D. M., and Haydon, D. A. (1971). *J. Membrane Biol*. **5**, 277–96.

Fricke, H., and Morse, S. (1925). *J. Gen. Physiol.* **9**, 153–67.

Israelachvili, J. N. (1977). *Biochim. Biophys. Acta* **469**, 221–5.
Israelachvili, J. N., Mitchell, D. J., and Ninham, B. W. (1976). *J. Chem. Soc. Faraday Trans. II* **72**, 1525–68.
Mahaworasilpa, T. L., Coster, H. G. L., and George, E. P. (1994). *Biochim. Biophys. Acta* **1193**, 118–26.
Markx, G. H., and Pethig, R. (1995). *Biotechnol. Bioeng.* **45**, 337–43.
Markx, G. H., Talary, M., and Pethig, R. (1994). *J. Biotechnology* **32**, 29–37.
Parsegian, A. (1969). *Nature* **221**, 844–6.
Pethig, R., and Markx, G. H. (1997). *Trends Biotech.* **15**, 426–32.
Robertson, J. D. (1960). *Prog. Biophys.* **10**, 343–418.
Singer, S. J., and Nicholson, G. L. (1972). *Science* **175**, 720–31.
Zimmermann, U., Beckers, F., and Coster, H. G. L. (1977). *Biochim. Biophys. Acta* **464**, 399–416.

Manuscript received 29 October 1998, accepted 3 February 1999